Available online at www.sciencedirect.com
SCIENCE DIRECT®
Developmental Biology 293 (2006) 370–381
DEVELOPMENTAL BIOLOGY
www.elsevier.com/locate/ydbio

Synergistic interaction between *Gdf1* and *Nodal* during anterior axis development

Olov Andersson, Eva Reissmann, Henrik Jörnvall, Carlos F. Ibáñez *

Division of Molecular Neurobiology, Department of Neuroscience, Karolinska Institutet, S-17177 Stockholm, Sweden

Received for publication 22 September 2005; revised 2 February 2006; accepted 3 February 2006
Available online 27 March 2006

Abstract

Growth and Differentiation Factor 1 (GDF-1) has been implicated in left–right patterning of the mouse embryo but has no other known function. Here, we demonstrate a genetic interaction between *Gdf1* and *Nodal* during anterior axis development. $Gdf1^{-/-};Nodal^{+/-}$ mutants displayed several abnormalities that were not present in either $Gdf1^{-/-}$ or $Nodal^{+/-}$ single mutants, including absence of notochord and prechordal plate, and malformation of the foregut; organizing centers implicated in the development of the anterior head and branchial arches, respectively. Consistent with these deficits, $Gdf1^{-/-};Nodal^{+/-}$ mutant embryos displayed a number of axial midline abnormalities, including holoprosencephaly, anterior head truncation, cleft lip, fused nasal cavity, and lack of jaws and tongue. The absence of these defects in single mutants indicated a synergistic interaction between Nodal and GDF-1 in the node, from which the axial mesendoderm that gives rise to the notochord, prechordal plate, and foregut endoderm originates, and where the two factors are co-expressed. This notion was supported by a severe downregulation of FoxA2 and goosecoid in the anterior primitive streak of double mutant embryos. Unlike that in the lateral plate mesoderm, Nodal expression in the node was independent of GDF-1, indicating that both factors act in parallel to control the development of mesendodermal precursors. Receptor reconstitution experiments indicated that GDF-1, like Nodal, can signal through the type I receptors ALK4 and ALK7. However, analysis of compound mutants indicated that ALK4, but not ALK7, was responsible for the effects of GDF-1 and Nodal during anterior axis development. These results indicate that GDF-1 and Nodal converge on ALK4 in the anterior primitive streak to control the formation of organizing centers that are necessary for normal forebrain and branchial arch development.

Keywords: ALK4; ALK7; TGFβ; Holoprosencephaly; Notochord; Axial mesendoderm; Branchial arch; Prechordal plate

Introduction

The most common malformation of the human forebrain is caused by defects in the anterior midline, resulting in holoprosencephaly (Roessler and Muenke, 2001). Several different signaling pathways have been implicated in forebrain development by either transducing instructive signals arising from the underlying prechordal plate or by being directly expressed in the developing forebrain (Monuki and Walsh, 2001). The prechordal plate constitutes the anterior end of the axial mesendoderm and is thought to promote ventral midline development by secreting Sonic hedgehog (Shh) and other inductive cues (Chiang et al., 1996; Kiecker and Niehrs, 2001; Stern, 2001). Nodal belongs to the Transforming Growth Factor-β (TGF-β) superfamily of ligands and has been shown to be necessary for the formation of the axial mesendoderm (Lowe et al., 2001), which specifies the notochord, prechordal plate, and anterior definitive endoderm (Camus et al., 2000; Vincent et al., 2003). Targeted deletion studies in mice have demonstrated that lack of Shh or reduced Nodal signaling results in holoprosencephaly (Chiang et al., 1996; Lowe et al., 2001). The importance of Shh and Nodal for the development of holoprosencephaly is also supported by genetic studies in humans (Roessler and Muenke, 2001). Moreover, mice that were trans-heterozygous for mutations in *Nodal* and *smad2*, which encodes a downstream mediator of Nodal signaling, displayed similar malformations (Nomura and Li, 1998). Together, these findings highlight

* Corresponding author. Fax: +46 8 33 9548.
E-mail address: carlos.ibanez@ki.se (C.F. Ibáñez).

0012-1606/$ - see front matter © 2006 Elsevier Inc. All rights reserved.
doi:10.1016/j.ydbio.2006.02.002

the importance of Nodal signaling during forebrain development but leave open the possibility that other ligands of the TGF-β superfamily – particularly those activating similar intracellular pathways – could converge with Nodal to jointly mediate these effects.

Members of the TGF-β superfamily include more than 30 different proteins that signal through a heteromeric receptor-complex consisting of type I and type II receptors with intrinsic serine–threonine kinase activity (Shi and Massague, 2003). Seven type I receptors – termed Activin Receptor-like Kinase (ALK) 1 to 7 – have been identified so far, which specify intracellular signaling into two major pathways by phosphorylating different sets of Smad proteins. The "funnel-like" structure of the TGF-β signaling network – i.e. 30 ligands → 7 type I receptors → 2 Smad pathways – suggests the existence of redundant and compensatory interactions between different ligands and receptors. We and others have previously shown that Nodal can signal via the type I receptors ALK4 and ALK7 (Reissmann et al., 2001; Yeo and Whitman, 2001). Expression of the GPI-anchored co-receptor Cripto is required for Nodal signaling via ALK4 and greatly enhances its signaling via ALK7 (Reissmann et al., 2001). However, since ALK4 mutant mice die at gastrulation (Gu et al., 1998), and ALK7 is dispensable for Nodal signaling during embryogenesis in mice (Jörnvall et al., 2004), the precise functions of these two receptors remain to be defined.

Reduced Nodal signaling gives rise to several abnormalities in addition to holoprosencephaly and anterior head truncation, including randomized left–right patterning and hyposplenia (Lowe et al., 2001). Left–right patterning malformations have also been observed in mice carrying a targeted deletion of Growth and Differentiation Factor 1 (GDF-1), another member of the TGF-β superfamily, which was explained by the observation that GDF-1 signaling is required for expression of Nodal in the lateral plate mesoderm (Rankin et al., 2000). Nodal expression is controlled by two distinct regulatory elements, one upstream enhancer that regulates expression in the node, and one intronic enhancer that regulates expression in the epiblast, visceral endoderm, and lateral plate mesoderm (Norris and Robertson, 1999). Since GDF-1 is crucial for expression of Nodal in the lateral plate mesoderm, it may also affect other expression domains of Nodal that are regulated by the intronic enhancer. A complex consisting of phosphorylated Smad 2 or 3 and the transcription factor Foxh1 can bind to the intronic enhancer, thereby establishing a positive feedback loop controlling *Nodal* gene expression (Dunn et al., 2004; Norris et al., 2002). GDF-1 has been shown to utilize similar receptors as Nodal, including ALK4, Cripto and ActRIIA or ActRIIB (Cheng et al., 2003). Thus, GDF-1 may synergize with Nodal by at least two – not mutually exclusive – mechanisms, namely reinforcing Nodal expression and activating a similar set of receptors and Smad proteins.

In this study, we investigated possible synergistic functions of GDF-1 and Nodal signaling by examining genetic interactions between the *Gdf1*, *Nodal*, *Alk4*, and *Alk7* genes in mutant mice. The results of these studies revealed novel functions for GDF-1 during anterior axis development.

Results

Genetic interaction between Gdf1 and Nodal during forebrain development

Mutant mice lacking Nodal die at gastrulation, whereas mice that are heterozygote for this mutation appear normal (Lowe et al., 2001). In order to examine possible genetic interactions between *Gdf1* and *Nodal*, we generated compound mutant mice that are heterozygote for the *Nodal* mutation and homozygote for a null allele of the *Gdf1* gene. A similar strategy has previously been exploited to reveal Nodal-dependent phenotypes in compound mutant mice carrying mutations in *ActRIIA*, *ActRIIB*, and *Smad2*, indicating that Nodal function is susceptible to gene-dosage effects (Nomura and Li, 1998; Oh and Li, 2002; Song et al., 1999). $Gdf1^{+/-}$ and $Gdf1^{+/-}$;$Nodal^{+/-}$ mice were bred to generate $Gdf1^{-/-}$;$Nodal^{+/-}$ offspring. A decline in the observed frequency of this genotype with respect to the expected Mendelian ratio was already detected at E13.5 (Table 1), indicating partial embryonic lethality during the second week of gestation. In contrast, $Gdf1^{-/-}$ single mutant embryos are viable up to at least E14.5 (our own observations and Rankin et al., 2000), which suggests an earlier onset of embryonic loss in the compound mutants.

The embryonic lethality of $Gdf1^{-/-}$;$Nodal^{+/-}$ embryos correlated with variable phenotypes that were not present in either $Gdf1^{-/-}$ or $Nodal^{+/-}$ single mutant littermates. Morphological analysis of affected $Gdf1^{-/-}$;$Nodal^{+/-}$ embryos revealed that they developed within the yolk sac and had paired somites as normal embryos. However, they failed to develop anterior neural folds, resembling the type I phenotype previously described in mice carrying a *Nodal* hypomorphic allele (Lowe et al., 2001). Holoprosencephaly, in association with gross rostral truncation and cleft lip, was observed in 68% of $Gdf1^{-/-}$;$Nodal^{+/-}$ embryos examined at E13.5 ($n = 19$) (Figs. 1C, D, F). Two embryos that showed split face and exencephaly, however, did not display holoprosencephaly (Fig. 1E). Embryos with holoprosencephaly showed a thickening of the diencephalon and a recessed third ventricle that failed to expand ventrally (Fig. 1G). No forebrain defects were detected in any $Gdf1^{-/-}$ or $Nodal^{+/-}$ single mutant mice (Fig. 1B and data not shown), indicating synergistic interactions between GDF-1 and Nodal during development of the forebrain.

Table 1
Observed frequency of $Gdf1^{-/-}$;$Nodal^{+/-}$ offspring obtained from crosses between $Gdf1^{+/-}$ females and $Gdf1^{+/-}$;$Nodal^{+/-}$ males

Age	Total obtained	$Gdf1^{-/-}$;$Nodal^{+/-}$ offspring observed	$Gdf1^{-/-}$;$Nodal^{+/-}$ offspring (%)
E6.5–7.5	120	16	13.33
E8.5	94	15	15.96
E9.5–10.5	131	18	13.74
E13.5	93	8	8.6
E18.5–P0	111	4	3.6
Total	549	61	11.11

Expected frequency was 12.5%.

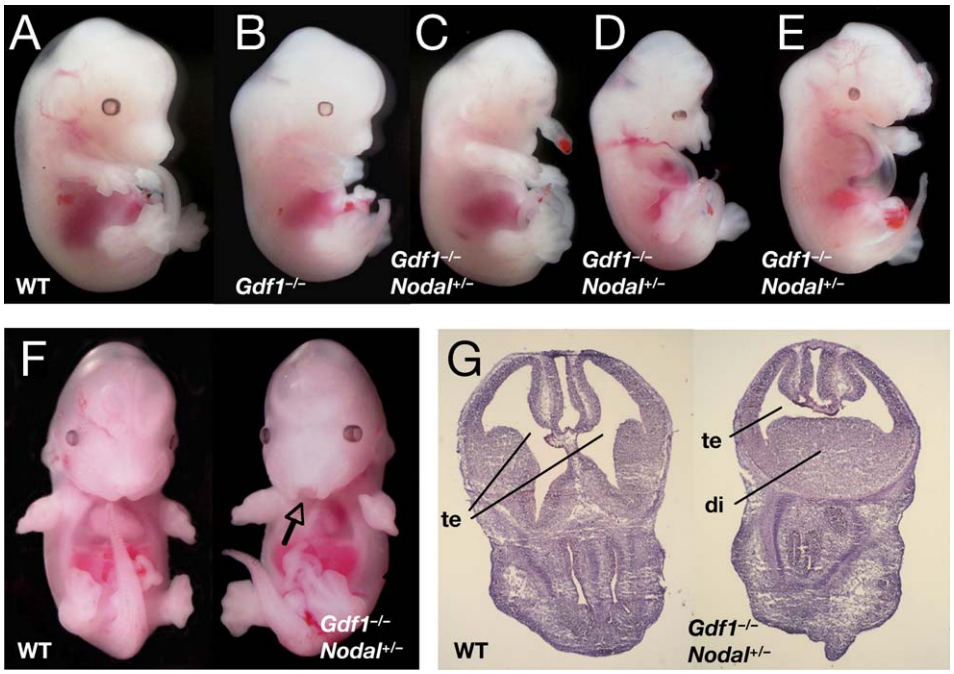

Fig. 1. Genetic interaction between *Gdf1* and *Nodal* during forebrain development. (A–E) Lateral views of wild-type (A), *Gdf1*$^{-/-}$ (B), and three *Gdf1*$^{-/-}$;*Nodal*$^{+/-}$ mutant (C–E) embryos at E13.5. Embryos shown in panels C and D display holoprosencephaly and anterior head truncation, while that in panel E exhibits split face with exencephaly. (F) Ventral view of wild-type and *Gdf1*$^{-/-}$;*Nodal*$^{+/-}$ mutant embryos at E13.5. Cleft lip in the mutant is indicate by an arrow. (G) Sections through wild-type and *Gdf1*$^{-/-}$;*Nodal*$^{+/-}$ mutant embryos at E13.5. The mutant brain shows a single forebrain vesicle and thickening of the diencephalon. di, diencephalon; te, telencephalon.

GDF-1 and Nodal are necessary for the development of the notochord and prechordal plate

In order to determine the mechanisms underlying anterior malformations in *Gdf1*$^{-/-}$;*Nodal*$^{+/-}$ mutant embryos, we examined the expression of a panel of markers at early stages of embryonic development using whole-mount in situ hybridization. FoxA2 (HNF3β) and Goosecoid (Gsc) are two markers of the anterior primitive streak, from which the axial mesendoderm is later derived, and have been shown to function synergistically in the specification of anterior mesendodermal precursors (Filosa et al., 1997). At mid-streak stage, *Gdf1*$^{-/-}$;*Nodal*$^{+/-}$ mutant embryos often showed decreased FoxA2 expression in the anterior primitive streak (88%, $n = 8$) (Fig. 2A), while Gsc expression was either greatly reduced or absent in this structure (100%, $n = 4$) (Fig. 2B). The elongation of the primitive streak in *Gdf1*$^{-/-}$;*Nodal*$^{+/-}$ mutant embryos was evaluated by examining the expression of Brachyury (T), which normally marks mesodermal cells along the primitive streak and axial mesendoderm that will later give rise to the notochord and prechordal plate. Although the elongation of the streak was not disrupted in *Gdf1*$^{-/-}$;*Nodal*$^{+/-}$ mutant embryos, the axial mesendoderm cells that normally migrate anteriorly from the node were greatly reduced in half of the mutant embryos examined (50%, $n = 8$) (Fig. 2C). Single mutant embryos for *Gdf1*$^{-/-}$ or *Nodal*$^{+/-}$ did not show defects in the anterior primitive streak or the axial mesendoderm (Figs. 2A, C). Together, these data indicate that GDF-1 and Nodal function synergistically in the anterior primitive streak to promote the formation of axial mesendoderm.

Nodal signaling has been shown to control the specification of axial mesendoderm precursors into progenitors of the prechordal plate and notochord (Rossant and Tam, 2004; Vincent et al., 2003). In order to assess the development of these structures in *Gdf1*$^{-/-}$;*Nodal*$^{+/-}$ mutant embryos, we examined the expression of gsc, T, Shh, and FoxA2 at different post-gastrulation stages. Gsc, a marker of the prechordal plate, was significantly downregulated in all *Gdf1*$^{-/-}$;*Nodal*$^{+/-}$ mutant embryos examined at late headfold stage (100%, $n = 4$) (Fig. 2D). At E8.5, expression of T could still be detected in the regressing primitive streak of mutant embryos but was often partially or completely missing in the notochord (44%, $n = 9$) (Fig. 2E). Sections through embryos stained with T confirmed that, while T expression in the regressing primitive streak appeared normal – or only slightly down-regulated (Figs. 2F, G) – the notochord was absent in the most severely affected *Gdf1*$^{-/-}$;*Nodal*$^{+/-}$ mutant embryos (Figs. 2H, I). At E9, expression of Shh – which normally marks the notochord at this stage – was anteriorly truncated in all *Gdf1*$^{-/-}$;*Nodal*$^{+/-}$ mutant embryos examined (100%, $n = 5$) (Fig. 3A). Axial mesendoderm is a potent inducer of floor-plate character in the overlying neural tube. Consistent with the absence of prechordal plate and notochord in *Gdf1*$^{-/-}$;*Nodal*$^{+/-}$ embryos, FoxA2 was significantly downregulated in the floor-plate of mutants showing anterior truncation (83%, $n = 6$) (Figs. 3B–D).

Specification of the neural plate in E8.5 *Gdf1*$^{-/-}$;*Nodal*$^{+/-}$ mutant embryos was evaluated by assessing expression of Six3, Engrailed-2 (En-2), and Krox20, which mark subpopulations of cells in the forebrain, midbrain, and hindbrain

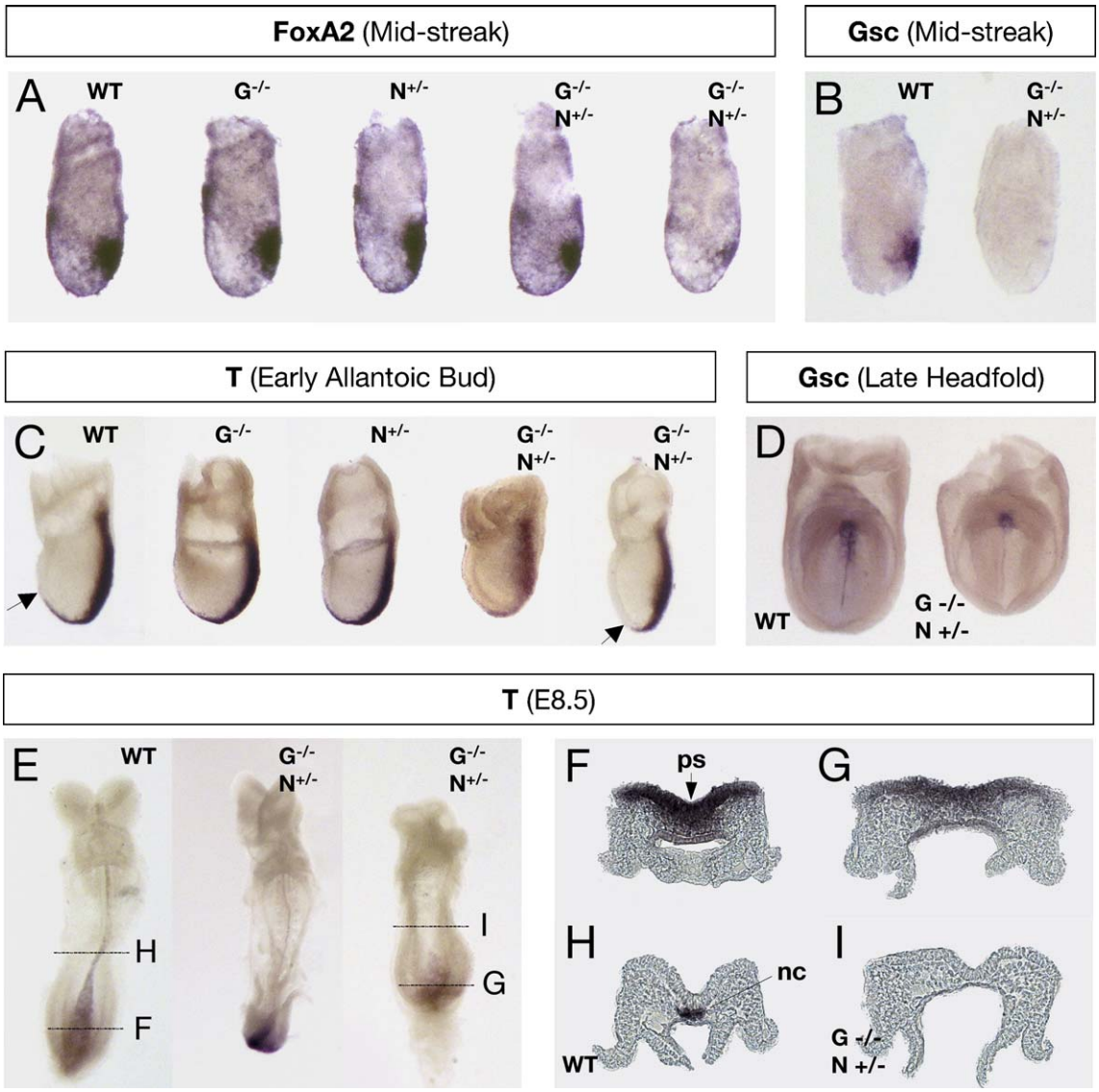

Fig. 2. GDF-1 and Nodal are necessary for the development of the notochord and prechordal plate. (A) FoxA2 expression in wild-type (WT), *Gdf1*$^{-/-}$ (G$^{-/-}$), *Nodal*$^{+/-}$ (N$^{+/-}$), and two *Gdf1*$^{-/-}$;*Nodal*$^{+/-}$ mutant (G$^{-/-}$;N$^{+/-}$) embryos at mid-streak stage. The anterior primitive streak marker FoxA2 (HNF3β, arrowhead) is differentially downregulated in the anterior primitive streak in *Gdf1*$^{-/-}$;*Nodal*$^{+/-}$ mutants, whereas normal expression is found in single mutants. (B) Gsc expression in wild-type and *Gdf1*$^{-/-}$;*Nodal*$^{+/-}$ mutant embryos at mid-streak stage. Gsc expression in the anterior primitive streak is absent in the mutant. (C) T expression in wild-type, *Gdf1*$^{-/-}$, *Nodal*$^{+/-}$, and two *Gdf1*$^{-/-}$;*Nodal*$^{+/-}$ mutant embryos at early allantoic bud stage. T normally marks mesodermal cells along the primitive streak and axial mesendoderm. While the staining in the streak was present in all embryos, a loss of T-expressing cells migrating anteriorly could be seen in approximately half of the *Gdf1*$^{-/-}$;*Nodal*$^{+/-}$ mutants examined (arrows point at the most anterior T-expressing cells). (D) Gsc expression in frontal views of wild-type and *Gdf1*$^{-/-}$;*Nodal*$^{+/-}$ mutant embryos at late headfold stage. Gsc is clearly downregulated in the prechordal plate of the mutants. (E) T expression in wild-type and two differently affected *Gdf1*$^{-/-}$;*Nodal*$^{+/-}$ mutant embryos at E8.5. (F–I) T expression in sections from wild-type (F, H) and *Gdf1*$^{-/-}$;*Nodal*$^{+/-}$ mutant (G, I) embryos through the planes indicated in panel E. While some expression of T in the regressing primitive streak (ps) could still be observed in both wild-type and mutant embryos (F, G), the notochord (nt) was absent in severely affected *Gdf1*$^{-/-}$;*Nodal*$^{+/-}$ mutants (compare H and I).

regions, respectively. Consistent with their abnormal anterior axial development, neural plate defects were restricted to the forebrain in *Gdf1*$^{-/-}$;*Nodal*$^{+/-}$ mutants. Thus, while expression of En-2 and Krox20 could be detected in all the mutants examined (100%, $n = 5$ and $n = 7$, respectively) (Figs. 3E, F), Six3 expression was variably affected, ranging from no difference to complete loss in the most affected embryos (43%, $n = 7$) (Fig. 3E). Although expression of Krox-20 in rhombomeres 3 and 5 appeared normal even in the most affected mutants (Fig. 3E), the expression domain of En-2 was tilted ventrally as a result of anterior truncations in the mutants (Fig. 3F). Thus, while the *Gdf1*$^{-/-}$;*Nodal*$^{+/-}$ mutation did not affect the overall regionalization of the neural plate, deficits in anterior axial development resulted in forebrain abnormalities of variable penetrance in the mutants. Together, the results from these analyses indicate that GDF-1 and Nodal function synergistically in the specification of the prechordal plate and notochord, which in turn are necessary for the normal development of anterior structures in the neural plate.

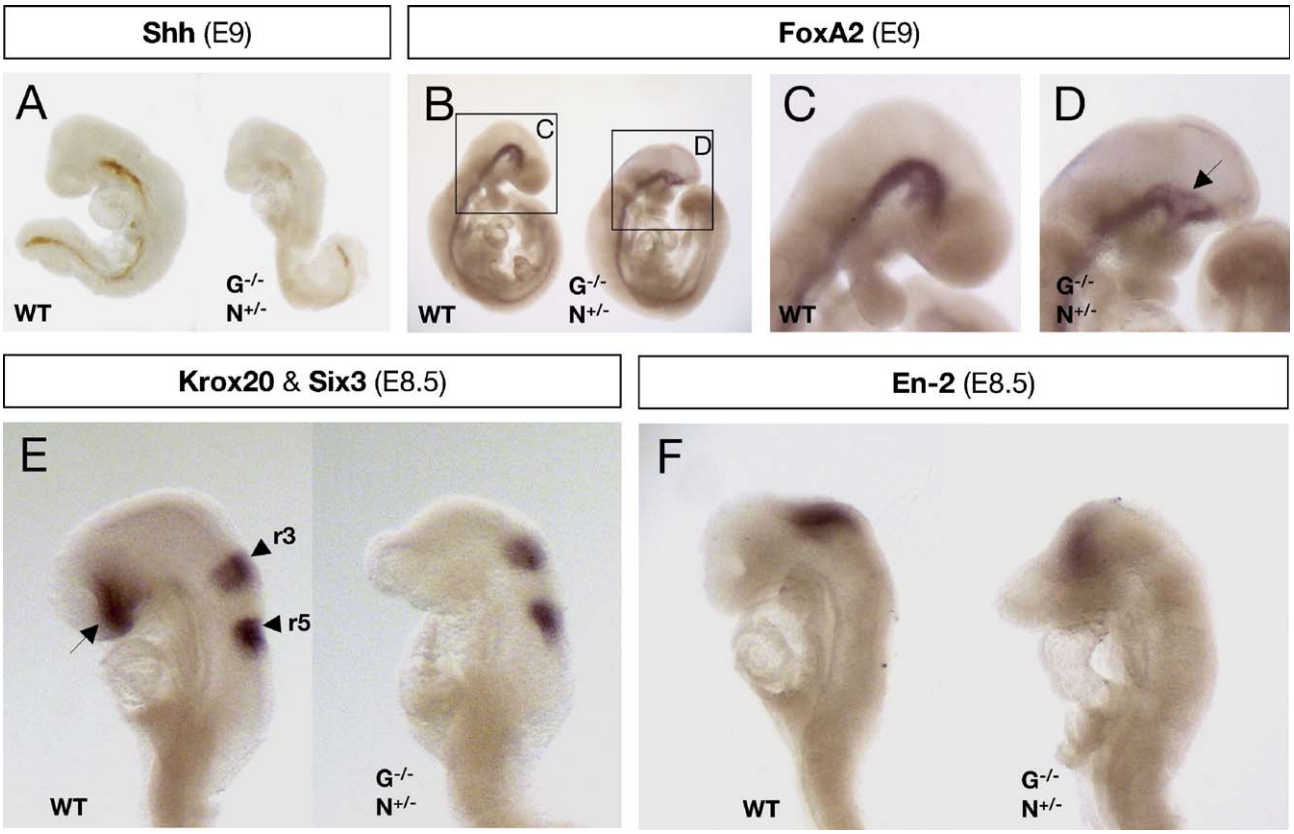

Fig. 3. Defects in anterior patterning of the floor plate and neural plate of *Gdf1*$^{-/-}$;*Nodal*$^{+/-}$ mutants. (A) Shh expression in the notochord of E9 wild-type (WT) and *Gdf1*$^{-/-}$;*Nodal*$^{+/-}$ mutant (G$^{-/-}$;N$^{+/-}$) embryos showing absence of Shh immunoreactivity in the anterior notochord of mutant embryos. (B) Expression of FoxA2 in the neural tube of E9 wild-type and *Gdf1*$^{-/-}$;*Nodal*$^{+/-}$ mutant embryos. (C, D) High magnification of regions boxed in panel B showing reduced FoxA2 expression in the floorplate of *Gdf1*$^{-/-}$;*Nodal*$^{+/-}$ mutant embryos (arrow). (E) Expression of Six3 and Krox20 in E8.5 wild-type and *Gdf1*$^{-/-}$;*Nodal*$^{+/-}$ mutant embryos. The forebrain marker Six3 was downregulated in *Gdf1*$^{-/-}$;*Nodal*$^{+/-}$ mutants that showed anterior truncation. The hindbrain marker Krox20 was unaffected in all embryos examined. (F) Expression of the midbrain and anterior hindbrain marker En-2 in E8.5 wild-type and *Gdf1*$^{-/-}$;*Nodal*$^{+/-}$ mutant embryos. r3, r5: rhombomeres 3 and 5.

Genetic interaction between Gdf1 and Nodal during development of the foregut endoderm and structures derived from the first branchial arch

The first branchial arch gives rise to the jaws, nasal septum, and distal parts of the tongue, whereas the second branchial arch gives rise to different structures such as the bony parts of the ear (Kontges and Lumsden, 1996). Defects in structures derived from the first branchial arch were observed in 67% of *Gdf1*$^{-/-}$;*Nodal*$^{+/-}$ mutant embryos examined between E10 and P0 (n = 15). Strongly affected embryos lacked both tongue and jaw as shown by the absence of mandibles in skeleton preparations (Figs. 4A–D). In mildly affected embryos, the distal part of the tongue was not formed, whereas the base of the tongue and jaw were still present (Figs. 4E, F). Other defects found in *Gdf1*$^{-/-}$;*Nodal*$^{+/-}$ mutants included a fused nasal cavity due to a hypomorphic nasal septum (Figs. 4G, H), which is a midline defect often associated with holoprosencephaly. No defects in structures arising from the second brachial arch could be detected, as indicated by a normal complement of ear bones (Fig. 4D). First branchial arch malformations did not always coincide with holoprosencephaly, suggesting that patterning of these two regions depend on independent signaling events.

In comparison to the forebrain, relatively less is known about the identity of the inductive signals involved in branchial arch formation. Previous studies have indicated that development of the first branchial arch into structures such as the jaw may depend upon signals from an organizing center located in the foregut endoderm (Couly et al., 2002; Kirby et al., 2003; Petryk et al., 2004; Zakin and De Robertis, 2004). Consistent with this notion, the rostral part of the foregut diverticulum widens laterally to form the first branchial pouch and is therefore in close proximity to the developing branchial arches. As the foregut endoderm is also a derivative of the axial mesendoderm (Tam and Beddington, 1992), we investigated possible abnormalities in foregut endoderm development in *Gdf1*$^{-/-}$;*Nodal*$^{+/-}$ mutant embryos by examining the expression of FoxA2 and Hex, two markers expressed during early foregut development. FoxA2 stains the foregut endoderm as it forms the foregut diverticulum, and was found to be downregulated in 50% of *Gdf1*$^{-/-}$;*Nodal*$^{+/-}$ embryos examined at E8.5 (n = 8) (Fig. 4I). On the other hand, Hex marks the foregut endoderm as it extends anteriorly and has been shown to control the proliferative rate of cells at the foregut leading edge and hence the overall growth of this structure (Bort et al., 2004). Hex expression was also found to be significantly reduced in the foregut diverticulum of E9 mutant embryos (80%, n = 5) (Figs.

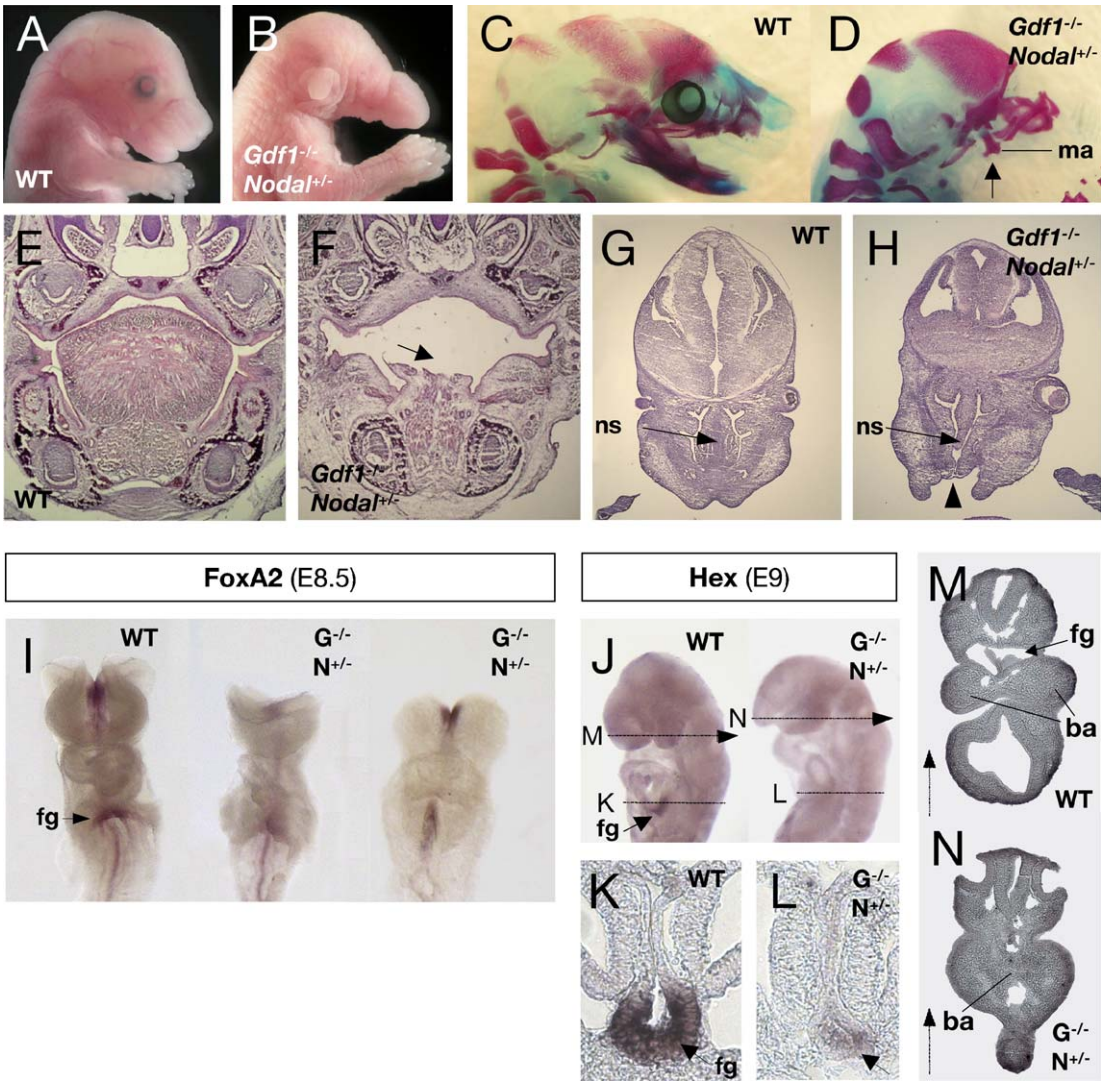

Fig. 4. Defects in foregut endoderm and structures derived from the first branchial arch in *Gdf1*$^{-/-}$;*Nodal*$^{+/-}$ mutant embryos. (A, B) Lateral views of wild-type (A) and *Gdf1*$^{-/-}$;*Nodal*$^{+/-}$ mutant (B) embryos at E18.5 showing gross malformations in anterior head structures in the mutant. (C, D) Skeleton stainings of skulls from embryos shown in panels A and B. Arrow in panel D denotes absence of jaws and skeletal structures beyond the malleus (ma) in the mutant skull. (E, F) Coronal sections through the anterior head of a newborn wild-type (E) and a mildly affected *Gdf1*$^{-/-}$;*Nodal*$^{+/-}$ mutant (F) showing absence of the distal part of the tongue (arrow in F) in the mutant. (G, H) Section of wild-type (G) and *Gdf1*$^{-/-}$;*Nodal*$^{+/-}$ mutant (H) heads at E13.5 showing cleft lip (arrowhead in H) and hypomorphic nasal septum (ns) resulting in fused nasal cavity in the mutant. (I) Expression of FoxA2 in E8.5 wild-type (WT) and two *Gdf1*$^{-/-}$;*Nodal*$^{+/-}$ mutants (G$^{-/-}$;N$^{+/-}$) embryos showing downregulation of FoxA2 in the foregut endoderm of the mutants. fg, foregut. (J) Expression of Hex in E9 wild-type and *Gdf1*$^{-/-}$;*Nodal*$^{+/-}$ mutant embryos showing downregulation of Hex expression in the foregut endoderm of the mutant (arrow). (K, L) Hex expression in sections from E9 wild-type (K) and *Gdf1*$^{-/-}$;*Nodal*$^{+/-}$ mutant (L) embryos through the planes indicated in panel J, showing reduced expression in the mutant foregut (fg, arrow). (M, N) Sections from E9 wild-type (M) and *Gdf1*$^{-/-}$;*Nodal*$^{+/-}$ mutant (N) embryos through the planes indicated in panel J (dotted arrows denote the orientation of the sections), showing anterior truncation of the foregut and fused first branchial arches in the mutant.

4J–L). Moreover, in more anterior sections, it could also be confirmed that in the majority of cases the foregut in E9 *Gdf1*$^{-/-}$;*Nodal*$^{+/-}$ embryos did not reach into the center of the first branchial arch as it did in wild-type embryos (Figs. 4M, N), confirming its anterior truncation up to the level of this structure (83%, n = 6). A similar defect has been observed in Smad2 mutant mice (Vincent et al., 2003). These sections also revealed that the first branchial arch was fused and lacked a midline division in *Gdf1*$^{-/-}$;*Nodal*$^{+/-}$ mutants (Figs. 4M, N). Together, these data are in agreement with a concomitant requirement of GDF-1 and Nodal signaling in the development of the foregut endoderm and structures derived from the first branchial arch.

Nodal expression outside the lateral plate mesoderm is independent of GDF-1

Next, we set out to establish the epistatic relationship between *Nodal* and *Gdf1* in the control of forebrain and branchial arch development. GDF-1 has been shown to act directly upstream of Nodal during left–right patterning of the mouse embryo by controlling Nodal expression in the lateral plate mesoderm (Rankin et al., 2000). Whether GDF-1 also regulates Nodal expression at other sites is currently unknown. In agreement with previous studies, we found that Nodal – as assessed by expression of a *lacZ* reporter inserted in the *Nodal*

locus – and GDF-1 were co-expressed in the node and left lateral plate mesoderm (Figs. 5A, B). Unlike Nodal, however, GDF-1 was also expressed in the right lateral plate mesoderm (Fig. 5B), despite the fact that both factors affect left–right patterning in a similar manner. GDF-1 and Nodal are also co-expressed throughout the epiblast (Collignon et al., 1996; Rankin et al., 2000; Wall et al., 2000). Nodal expression has also been detected in the roofplate of the forebrain and in a small group of cells located at the border between the first and second branchial arches at E9.5 (Varlet et al., 1997a). This group of cells contributes to the first branchial pouch that will later give rise to the middle ear. However, GDF-1 is unlikely to exert a direct control over Nodal expression in those structures as it is not itself expressed in branchial arches or forebrain at that stage of development (Wall et al., 2000).

In order to assess the extent to which GDF-1 controls Nodal expression in different regions of the developing mouse embryo, we compared the activity of the *lacZ* reporter gene inserted into the *Nodal* locus in *Nodal*$^{+/-}$ heterozygous and *Gdf1*$^{-/-}$;*Nodal*$^{+/-}$ double mutants. β-gal activity in early streak stages was not affected by the lack of GDF-1 (n = 7) (Fig. 5C), indicating that GDF-1 does not act upstream of Nodal in this structure. In agreement with previous results, β-gal activity was drastically reduced in the lateral plate mesoderm of *Gdf1*$^{-/-}$;*Nodal*$^{+/-}$ mutants at E8 (5–8 somite embryos) (Rankin et al., 2000) but was still detected in the node (n = 7) (Fig. 5D). We could neither detect any reduction in β-gal activity in the first branchial pouch of *Gdf1*$^{-/-}$;*Nodal*$^{+/-}$ mutants compared to *Nodal*$^{+/-}$ embryos, despite the obvious malformation of the first branchial arch in the double mutants (n = 5) (Figs. 5E, F). Likewise, β-gal activity could still be detected in the roofplate of *Gdf1*$^{-/-}$;*Nodal*$^{+/-}$ mice that displayed overt holoprosencephaly (n = 5) (Figs. 5G, H), indicating that the onset and maintenance of Nodal expression in this structure is

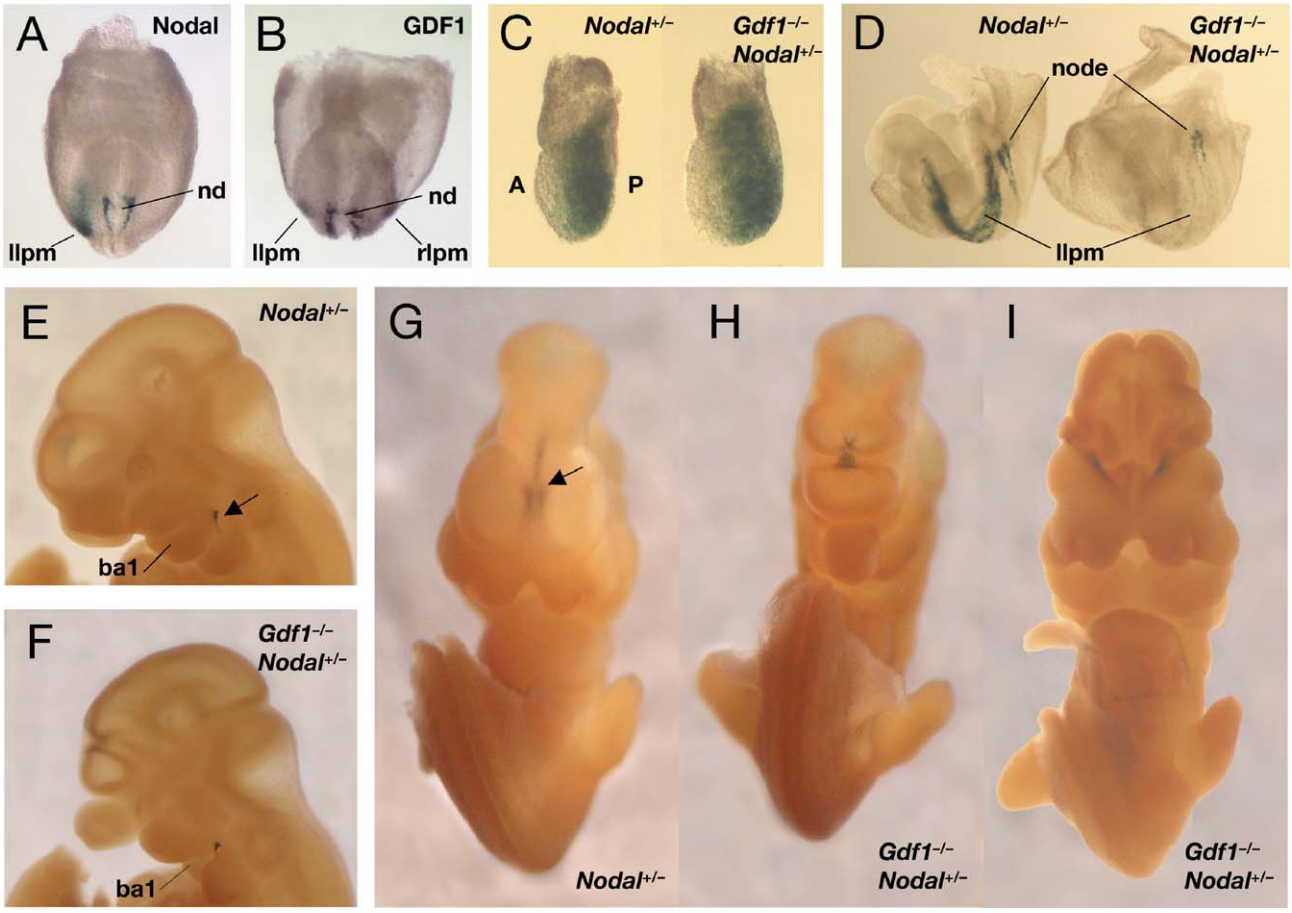

Fig. 5. Nodal expression outside the lateral plate mesoderm is independent of GDF-1. (A) *Nodal* expression in the node (nd) and left side of the lateral plate mesoderm (llpm) in a *Nodal*$^{+/-}$ late headfold stage embryo as assessed by β-gal staining. (B) *Gdf-1* expression in the node and left and right lateral plate mesoderm (llpm and rlpm, respectively) in a wild-type late headfold stage embryo as assessed by in situ hybridization. (C) *Nodal* expression at early streak stage in the epiblast of *Nodal*$^{+/-}$ and *Gdf1*$^{-/-}$;*Nodal*$^{+/-}$ embryos as assessed by β-gal activity. No downregulation of Nodal expression could be seen in the absence of GDF-1. A, anterior; P, posterior. (D) At E8 (5–8 somite embryos), β-gal activity was downregulated in the left lateral plate mesoderm of *Nodal*$^{+/-}$ mutant embryos lacking GDF-1, but no significant downregulation could be detected in the node. (E, F) At E10, Nodal is expressed in the first branchial pouch at the border between the first and the second branchial arches (arrow in E). Nodal expression in this structure is not affected by the absence of GDF-1 as assessed by comparing β-gal activity between *Nodal*$^{+/-}$ (E) and *Gdf1*$^{-/-}$;*Nodal*$^{+/-}$ (F) embryos. Note the reduced size of the first branchial arch in the mutant (F). ba1, branchial arch 1. (G–I) Nodal is expressed in the forebrain roofplate at E10 in *Nodal*$^{+/-}$ (G, arrow) and *Gdf1*$^{-/-}$;*Nodal*$^{+/-}$ (H, I) embryos. In a *Gdf1*$^{-/-}$;*Nodal*$^{+/-}$ embryo with holoprosencephaly (H), β-gal activity did not extend into the forebrain vesicle as observed in *Nodal*$^{+/-}$ counterparts. In a *Gdf1*$^{-/-}$;*Nodal*$^{+/-}$ embryo with exencephaly (I), β-gal activity could still be detected, but remained confined to the edges of the neural tube that did not close.

independent of GDF-1. Normal levels of β-gal activity could also be detected in one *Gdf1*$^{-/-}$;*Nodal*$^{+/-}$ embryo with exencephaly but in an abnormal pattern, confined to the edges of the neural tube that did not close (Fig. 5I). Thus, we conclude that, although GDF-1 is upstream of Nodal in the lateral plate mesoderm, it is dispensable for Nodal expression in the epiblast, node, forebrain roofplate, and first branchial arch, indicating that the two factors act in parallel to control the development of those structures.

GDF-1 and Nodal can signal through either ALK4 or ALK7 in vitro, but utilize ALK4 in vivo

GDF-1 has previously been shown to signal via the type I receptor ALK4 in collaboration with the type II receptors ActRIIA or ActRIIB, resulting in phosphorylation of Smad2 and Smad3 (Cheng et al., 2003). On the other hand, Nodal has been shown to utilize either ALK4 or ALK7 in complex with the same type II receptors (Reissmann et al., 2001; Yeo and Whitman, 2001). The similarity of GDF-1 and Nodal signaling prompted us to examine whether GDF-1 may also signal through ALK7 in collaboration with ActRIIB. Receptor activity was monitored in the human hepatoma cell line HepG2 transfected with expression plasmids for GDF-1 and the appropriate receptors, together with reporter constructs carrying the promoter from the Plasminogen Activator Inihitor-1 (PAI-1) gene upstream of a luciferase gene (p3TP-luc) or only the Smad3-binding element of the PAI-1 promoter repeated twelve times upstream of the luciferase gene (CAGA-luc) (Dennler et al., 1998). Significant reporter activity could only be seen following transfection of GDF-1 together with both ALK7 and ActRIIB (Fig. 6A). Using the CAGA-luc construct, the same receptor combination could be activated in a dose-dependent manner by co-transfected GDF-1 (Fig. 6B). Thus, similar to Nodal, GDF-1 can use ALK7 in collaboration with ActRIIB to activate Smad3-dependent reporter genes.

In order to determine which type I receptor mediates the effects of GDF-1 and Nodal signaling during anterior axis development, we generated compound mutant mice that were triple heterozygote for *Gdf1*, *Nodal*, and *Alk4* (*Gdf1*$^{+/-}$;*Nodal*$^{+/-}$;*Alk4*$^{+/-}$) or *Gdf1*, *Nodal* and *Alk7* (*Gdf1*$^{+/-}$;*Nodal*$^{+/-}$;*Alk7*$^{+/-}$), and assessed whether the mutant receptor alleles

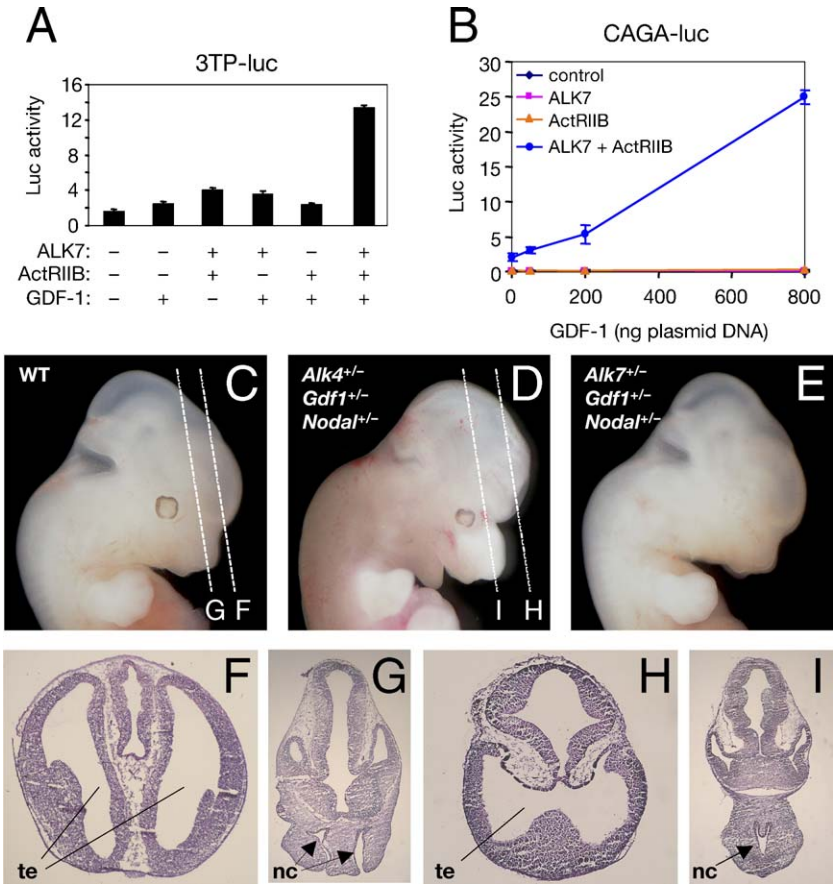

Fig. 6. GDF-1 and Nodal can signal through either ALK4 or ALK7 in vitro but utilize ALK4 in vivo. (A) Receptor reconstitution experiments in HepG2 cells show that GDF-1 can activate 3TP-luc five-fold when both ALK7 and ActRIIB are co-transfected but not when only one receptor is present. Results represent relative luciferase activity of triplicate determinations ± SD. The amounts of transfected plasmid DNA per three wells were 750 ng, 1 ng, and 0.2 ng, for GDF-1, ALK7, and ActRIIB, respectively. (B) Dose-dependent activation by the same combination of receptors using another reporter plasmid, i.e., CAGA-luc. Results represent relative luciferase activity of triplicate determinations ± SD. (C–E) Comparison of E12.5 wild-type (C), *Gdf1*$^{+/-}$;*Nodal*$^{+/-}$;*Alk4*$^{+/-}$ (D), and *Gdf1*$^{+/-}$;*Nodal*$^{+/-}$;*Alk7*$^{+/-}$ (E) embryos. (F–I) Sections from embryos as indicated in panels C and D. Wild-type embryos have a clear division of forebrain vesicles (F), and nasal cavities (G), whereas *Gdf1*$^{+/-}$;*Nodal*$^{+/-}$;*Alk4*$^{+/-}$ mutants have a single forebrain vesicle (H), and a fused nasal cavity (I), thus resembling the phenotype of *Gdf1*$^{-/-}$;*Nodal*$^{+/-}$embryos. te, telencephalon; nc, nasal cavity.

influenced the appearance of anterior axis defects in these mice. Three out of 19 *Gdf1*$^{+/-}$;*Nodal*$^{+/-}$;*Alk4*$^{+/-}$ mutant embryos were found to resemble some of the phenotypes seen in *Gdf1*$^{-/-}$;*Nodal*$^{+/-}$ double mutants, while none of the 16 *Gdf1*$^{+/-}$;*Nodal*$^{+/-}$;*Alk7*$^{+/-}$ mutant embryos examined revealed any abnormal phenotype (Figs. 6C–E). Sections of affected *Gdf1*$^{+/-}$;*Nodal*$^{+/-}$;*Alk4*$^{+/-}$ embryos clearly showed a single forebrain vesicle and a fused nasal cavity (Figs. 6F–I). No malformations were seen in any embryo with a lower number of mutant alleles.

The relative low incidence of malformations in *Gdf1*$^{+/-}$;*Nodal*$^{+/-}$;*Alk4*$^{+/-}$ triple heterozygous suggested that there were significant compensations by the remaining alleles, and prompted us to examine *Gdf1*$^{-/-}$;*Alk4*$^{+/-}$ double mutant embryos in which GDF-1 was totally absent. Indeed, *Gdf1*$^{-/-}$;*Alk4*$^{+/-}$ mutants more closely resembled *Gdf1*$^{-/-}$;*Nodal*$^{+/-}$ mutants, with 33% (3 out of 9) *Gdf1*$^{-/-}$;*Alk4*$^{+/-}$ embryos displaying anterior truncations, holoprosencephaly, and – in one case – cyclopia at E13.5 (Figs. 7A–C). In order to establish whether these abnormalities originated in early deficits similar to those observed in *Gdf1*$^{-/-}$;*Nodal*$^{+/-}$ mutants, we examined expression of FoxA2 in the anterior primitive streak, and T in primitive streak and axial mesendoderm. In agreement with our observations in *Gdf1*$^{-/-}$;*Nodal*$^{+/-}$ embryos, FoxA2 was significantly downregulated in the anterior primitive streak of all *Gdf1*$^{-/-}$;*Alk4*$^{+/-}$ mutants examined (100%, n = 7) (Fig. 7D). Moreover, we found decreased expression of T in the axial mesendoderm in a subset of *Gdf1*$^{-/-}$;*Alk4*$^{+/-}$ mutant embryos (30%, n = 10) (Fig. 7E). Single mutants for *Gdf1*$^{-/-}$ or *Alk4*$^{+/-}$ did not show decreased expression of FoxA2 or T (Figs. 7D, E), supporting a synergistic interaction between *Gdf1* and *Alk4*. Thus, these data indicate that similar developmental abnormalities underlie the phenotypes of *Gdf1*$^{-/-}$;*Alk4*$^{+/-}$ and *Gdf1*$^{-/-}$;*Nodal*$^{+/-}$ mutant embryos. We also generated a number of *Gdf1*$^{-/-}$;*Alk7*$^{-/-}$ compound mutants which however did not show any of the phenotypes described in this study (data not shown), supporting the notion that ALK7 is dispensable for Nodal and GDF-1 signaling during embryogenesis.

Expression of ALK4 has previously been described in detail during primitive streak stages (Gu et al., 1998), and it is possible that GDF-1 and Nodal signal exclusively via ALK4 during gastrulation due to a more restricted expression of ALK7. We therefore examined ALK7 expression during primitive streak stages using both in situ hybridization and the activity of the *lacZ* reporter gene inserted into the *Alk7* locus of mutant mice (Jörnvall et al., 2004). However, the expression of ALK7 was below the limit of detection (data not shown), which suggests that ALK4, and not ALK7, may be indispensable for GDF-1 and Nodal signaling during gastrulation due to its specific temporal and spatial expression pattern. Together, our results suggest that, although both Nodal and GDF-1 can interact with ALK7, their signaling in vivo during anterior axis development is mediated by ALK4. Moreover, the fact that *Nodal*-like phenotypes could be obtained in *Gdf1*$^{-/-}$;*Alk4*$^{+/-}$ mutants despite having a wild-type complement of *Nodal* alleles indicates that GDF-1 can contribute independently of Nodal to the activation of ALK4 receptors during patterning of anterior structures.

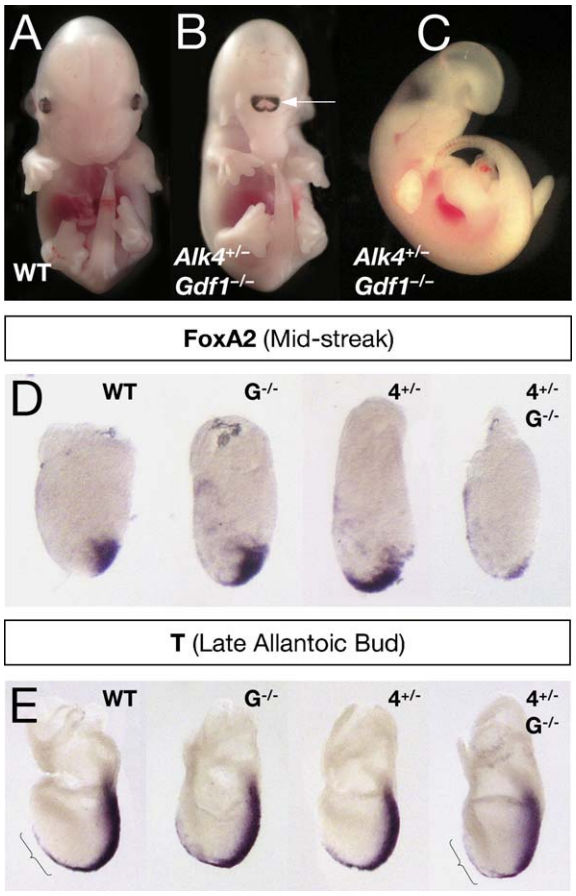

Fig. 7. *Gdf1*$^{-/-}$;*Alk4*$^{+/-}$ mutant embryos phenocopy the *Gdf1*$^{-/-}$;*Nodal*$^{+/-}$ mutation. (A to C) Frontal views of E13.5 wild-type (A) and *Gdf1*$^{-/-}$;*Alk4*$^{+/-}$ mutant (B, C) embryos. Cyclopia (arrow in B) and severe anterior truncations were observed in 3 out of 9 *Gdf1*$^{-/-}$;*Alk4*$^{+/-}$ double mutant embryos but never in the corresponding single mutants. (D) FoxA2 expression in mid streak wild-type (WT), *Gdf1*$^{-/-}$ (G$^{-/-}$), *Alk4*$^{+/-}$ (4$^{+/-}$), and *Gdf1*$^{-/-}$;*Alk4*$^{+/-}$ (4$^{+/-}$;G$^{-/-}$) mutant embryos. Similar to *Gdf1*$^{-/-}$;*Nodal*$^{+/-}$ mutants, expression of FoxA2 was decreased in the anterior primitive streak of *Gdf1*$^{-/-}$;*Alk4*$^{+/-}$ mutants compared to wild type. (E) T expression in wild-type, *Gdf1*$^{-/-}$, *Alk4*$^{+/-}$, and *Gdf1*$^{-/-}$;*Alk4*$^{+/-}$ mutant embryos at late allantoic bud stage. Note the partial loss of T expression in the axial mesendoderm of the *Gdf1*$^{-/-}$;*Alk4*$^{+/-}$ mutant (brackets), phenocopying the effects of the *Gdf1*$^{-/-}$;*Nodal*$^{+/-}$ mutation on this structure.

Discussion

GDF-1 collaborate with Nodal during embryogenesis

In this study, we describe several phenotypes associated with loss of GDF-1 and reduced Nodal signaling during mouse development. These malformations have previously been observed in mice carrying mutations in components of the Nodal signaling pathway and therefore thought to be exclusively due to perturbations in Nodal function. The transcription factor FoxH1 has been shown to be the major mediator of Nodal signaling during embryogenesis (Hoodless et al., 2001; Yamamoto et al., 2001). It is likely that GDF-1 signaling also relies on FoxH1 activity in the anterior primitive streak, since

malformations found in a subset of FoxH1 mutant embryos (i.e., type I embryos) are similar to those we found in *Gdf1*$^{-/-}$;*Nodal*$^{+/-}$ embryos. FoxH1 mutants differ however from *Gdf1*$^{-/-}$;*Nodal*$^{+/-}$ embryos in that elongation of the primitive streak is impaired in the former but not in the latter, as a consequence of FoxH1 ability to maintain *Nodal* expression in the anterior portion of the streak (Yamamoto et al., 2001). It is possible that this *Nodal-FoxH1* positive feedback loop is to a large extent cell autonomous, and that GDF-1 may not be able to affect it if expressed in nearby cells. The fact that primitive streak elongation proceeds normally in *Gdf1*$^{-/-}$;*Nodal*$^{+/-}$ embryos is consistent with *Nodal* expression in the streak and node being independent from GDF-1.

Gdf1$^{-/-}$;*Nodal*$^{+/-}$ *compound mutants display defects in derivatives of the anterior primitive streak*

FoxA2 is required during formation of the node, midline, and invagination of the foregut (Ang and Rossant, 1994). During gut formation, cells from the definitive endoderm migrate anteriorly from the anterior primitive streak to displace the visceral endoderm and form the foregut diverticulum. Consistent with a downregulation of FoxA2 in the anterior primitive streak, and of FoxA2 and Hex in the definitive endoderm, a restricted foregut invagination was observed in *Gdf1*$^{-/-}$;*Nodal*$^{+/-}$ mutants. This phenotype has previously been detected in *FoxH1*, *Smad2*, and chimeric *Nodal*$^{-/-}$ mutant embryos (Hoodless et al., 2001; Varlet et al., 1997b; Vincent et al., 2003). The fact that the foregut diverticulum still forms despite poor specification of the definitive endoderm has been attributed to the contribution of cells derived from the visceral endoderm to the gut tube. It is therefore possible that the foregut in *Gdf1*$^{-/-}$;*Nodal*$^{+/-}$ mutant embryos is at least in part populated by cells derived from the visceral endoderm.

Deletion of Gsc results in numerous of craniofacial malformations, but no gastrulation or axial defects (Rivera-Perez et al., 1995; Yamada et al., 1995). However, Gsc has been shown to genetically interact with FoxA2 in the anterior primitive streak of *Gsc*$^{-/-}$;*FoxA2*$^{+/-}$ mutants, resulting in defects in the foregut, forebrain and branchial arches (Belo et al., 1998; Filosa et al., 1997). Similar defects have also been observed in *FoxA2*$^{+/-}$;*Nodal*$^{+/-}$ mutants (Collignon et al., 1996) – but not in *Gsc*$^{-/-}$;*Nodal*$^{+/-}$ mutant embryos (Belo et al., 1998) – suggesting that there is a fine balance of signaling strength in which both ligands and transcription factors interact to specify derivatives of the anterior primitive streak. It would therefore be interesting to examine genetic interactions between *Gdf1*, *FoxA2*, and *Gsc* to elucidate the degree to which GDF-1 may act independently of Nodal during gastrulation.

Similarities and differences between GDF-1 and Vg1 orthologs

GDF-1 has been proposed to be a mammalian ortholog of *Xenopus*, chicken, and zebrafish Vg1, due to their sequence similarity and the fact that both GDF-1 and Vg1 regulate left–right patterning (Wall et al., 2000). Moreover, GDF-1 can induce mesendoderm and axial duplication when expressed in *Xenopus* embryos, thereby mimicking Vg1 function (Wall et al., 2000). In *Xenopus* embryos, studies with a dominant negative mutant form of Vg1 and with antisense constructs support a requirement for this protein in organizer maintenance during gastrulation and mesoderm induction (Birsoy et al., 2006; Joseph and Melton, 1998). Importantly, these experiments also suggested that the initial induction of the organizer can take place in the absence of Vg1. In contrast, Vg1 has been proposed to act upstream of Nodal during induction of the organizer in chick embryos (Skromne and Stern, 2001). Misexpression of Vg1 in the marginal zone of avian embryos has been shown to induce primitive streak formation, and co-expression with Wnt resulted in ectopic primitive streaks (Skromne and Stern, 2001). Thus, it seems that the requirement of Vg1/GDF-1 signaling during gastrulation differs between species; this variability may in turn depend upon different degrees of synergy between Nodal and its related factors.

GDF-1 and Nodal act in a dose-dependent fashion

Previous analyses of *Gdf1*$^{-/-}$ mutants had demonstrated the role of this factor in left–right patterning but did not reveal any abnormalities in anterior axis formation (Rankin et al., 2000). Our results indicate that GDF-1 contributes to the normal development of anterior structures together with Nodal, demonstrating how ligands and receptors of the TGF-β superfamily can collaborate to form a robust signaling network. GDF-1's contribution could be revealed by reducing Nodal signaling in compound mutant mice, in which GDF-1 then became necessary for the formation of the prechordal plate, notochord, and foregut endoderm. While evaluating left–right patterning defects in our colony, we detected a 20% incidence of right pulmonary isomerism in *Gdf1*$^{+/-}$;*Nodal*$^{+/-}$ double heterozygotes but none among the single mutants (data not shown), reflecting the synergistic interaction of the two factors during left–right patterning. Unlike *Gdf1*$^{-/-}$;*Nodal*$^{+/-}$ mutants, however, no forebrain or branchial arch malformations could be detected in the double heterozygote mutants, indicating that higher levels of combined Nodal/GDF-1 signaling are required for appropriate left–right patterning than for anterior axis development. This is in agreement with previous observations on the importance of graded Nodal signaling for the selective allocation of axial mesendoderm precursors during the formation of the anterior definitive endoderm and prechordal mesoderm (Vincent et al., 2003). The importance of dose-dependent Nodal signaling may also underlie the phenotypic variability observed in *Gdf1*$^{-/-}$;*Nodal*$^{+/-}$ embryos. It is possible that *Gdf1* expression may normally help to buffer intrinsic variability in *Nodal* levels that could otherwise arise from its complex regulation, which includes a potent positive feedback loop. In the absence of GDF-1, a single *Nodal* allele may only occasionally reach the signal strength threshold that is required for normal development.

Unlike the situation in the lateral plate mesoderm, Nodal expression in the node, epiblast, forebrain roofplate, and branchial arches was not dependent on GDF-1, indicating that GDF-1 does not act upstream of Nodal during the formation of

these structures, but rather that both factors contribute in parallel to anterior axis development. Together with previous work, our present results suggest that Nodal and GDF-1 cooperate to promote different biological effects in a dose-dependent fashion, thereby extending the notion of graded signaling to encompass the effects of two different factors that converge on a common set of receptors and intracellular mediators. Given their high degree of convergence on a limited set of receptors and signaling proteins, this mode of action may be widespread among several other members of the TGF-β superfamily.

Experimental procedures

Mouse strains and PCR primers

All mutant mice used in this study have previously been described in detail (Collignon et al., 1996; Gu et al., 1998; Jörnvall et al., 2004; Rankin et al., 2000). Nodal, Alk4, and Alk7 mutants were made in Sv129 substrains CCE, J1, and OlaHsd, respectively, whereas Gdf1 mutants were made in a Sv129; C57BL/6 hybrid strain. Littermates were used as controls in all experiments. Embryos were staged according to morphological landmarks described by Downs and Davies during early post-implantation development (Downs and Davies, 1993) and from E8.5 onwards according to the time at which they were harvested. Embryos were genotyped by PCR using the following sets of primers: Nodal targeted allele 5′-CTGTGCTCGACGTTGTCACTG-3′ and 5′-CTGGATGTAGGCATGGTTGGTAGGAT-3′, Alk4 targeted allele 5′-CTTGTCTGCAGCCAGTGGT-3′ and 5′-CCTCTGAGCCCAGAAAGC-GAAGG-3′, Alk7 targeted allele 5′-CGCCCCGGGAACTTCAAAGC-3′ and 5′-TAACAACCCGTCGGATTCTC-3′, Gdf1 wild-type allele 5′-TCGAA-GAAGAGCACGGAGAT-3′ and 5′-ATGTGAGCTTCCGTGAGGTG-3′, Gdf1 targeted allele 5′-CCACTGCAGCCTGTGGGCGC-3′ and 5′-GGAA-GACAATAGCAGGCATGCTGG-3.

Histology and receptor reconstitution experiments

Hematoxylin and eosin staining, X-gal staining, whole-mount in situ hybridization, and whole-mount immunostaining were performed according to standard protocols. All markers were digoxigenin labeled RNA probes, except in the case for Shh where a monoclonal antibody against Shh (clone 5E1, Developmental studies Hybridoma Bank) was used. Skeletal staining was performed as described (Oh and Li, 1997). Receptor reconstitution and reporter gene experiments were performed as described (Reissmann et al., 2001).

Acknowledgments

We are grateful to E. Robertson, E. Li, and S.J. Lee for providing *Nodal*, *Alk4*, and *Gdf1* mutant mice, respectively; E. M. De Robertis, B.G. Herrmann, B. Hogan, D. Kessler, J. Massagué, P. Tam, and P. ten Dijke for providing plasmids, and Carolina Svensson for secretarial help. This work was supported by grants from the Swedish Foundation for Strategic Research, the Swedish Cancer Society (3474-B97-05XBC), the Swedish Research Council (33X-10908-10A), and Hedlunds Stiftelse. E. R. was partially supported by a Marie Curie fellowship.

References

Ang, S.L., Rossant, J., 1994. HNF-3 beta is essential for node and notochord formation in mouse development. Cell 78, 561–574.

Belo, J.A., Leyns, L., Yamada, G., De Robertis, E.M., 1998. The prechordal midline of the chondrocranium is defective in Goosecoid-1 mouse mutants. Mech. Dev. 72, 15–25.

Birsoy, B., Kofron, M., Schaible, K., Wylie, C., Heasman, J., 2006. Vg 1 is an essential signaling molecule in *Xenopus* development. Development 133, 15–20.

Bort, R., Martinez-Barbera, J.P., Beddington, R.S., Zaret, K.S., 2004. Hex homeobox gene-dependent tissue positioning is required for organogenesis of the ventral pancreas. Development 131, 797–806.

Camus, A., Davidson, B.P., Billiards, S., Khoo, P., Rivera-Perez, J.A., Wakamiya, M., Behringer, R.R., Tam, P.P., 2000. The morphogenetic role of midline mesendoderm and ectoderm in the development of the forebrain and the midbrain of the mouse embryo. Development 127, 1799–1813.

Cheng, S.K., Olale, F., Bennett, J.T., Brivanlou, A.H., Schier, A.F., 2003. EGF-CFC proteins are essential coreceptors for the TGF-beta signals Vg1 and GDF1. Genes Dev 17, 31–36.

Chiang, C., Litingtung, Y., Lee, E., Young, K.E., Corden, J.L., Westphal, H., Beachy, P.A., 1996. Cyclopia and defective axial patterning in mice lacking Sonic hedgehog gene function. Nature 383, 407–413.

Collignon, J., Varlet, I., Robertson, E.J., 1996. Relationship between asymmetric nodal expression and the direction of embryonic turning. Nature 381, 155–158.

Couly, G., Creuzet, S., Bennaceur, S., Vincent, C., Le Douarin, N.M., 2002. Interactions between Hox-negative cephalic neural crest cells and the foregut endoderm in patterning the facial skeleton in the vertebrate head. Development 129, 1061–1073.

Dennler, S., Itoh, S., Vivien, D., ten Dijke, P., Huet, S., Gauthier, J.M., 1998. Direct binding of Smad3 and Smad4 to critical TGF beta-inducible elements in the promoter of human plasminogen activator inhibitor-type 1 gene. EMBO J. 17, 3091–3100.

Downs, K.M., Davies, T., 1993. Staging of gastrulating mouse embryos by morphological landmarks in the dissecting microscope. Development 118, 1255–1266.

Dunn, N.R., Vincent, S.D., Oxburgh, L., Robertson, E.J., Bikoff, E.K., 2004. Combinatorial activities of Smad2 and Smad3 regulate mesoderm formation and patterning in the mouse embryo. Development 131, 1717–1728.

Filosa, S., Rivera-Perez, J.A., Gomez, A.P., Gansmuller, A., Sasaki, H., Behringer, R.R., Ang, S.L., 1997. Goosecoid and HNF-3beta genetically interact to regulate neural tube patterning during mouse embryogenesis. Development 124, 2843–2854.

Gu, Z., Nomura, M., Simpson, B.B., Lei, H., Feijen, A., van den Eijnden-van Raaij, J., Donahoe, P.K., Li, E., 1998. The type I activin receptor ActRIB is required for egg cylinder organization and gastrulation in the mouse. Genes Dev. 12, 844–857.

Hoodless, P.A., Pye, M., Chazaud, C., Labbe, E., Attisano, L., Rossant, J., Wrana, J.L., 2001. FoxH1 (Fast) functions to specify the anterior primitive streak in the mouse. Genes Dev. 15, 1257–1271.

Jörnvall, H., Reissmann, E., Andersson, O., Mehrkash, M., Ibáñez, C.F., 2004. ALK7, a receptor for nodal, is dispensable for embryogenesis and left–right patterning in the mouse. Mol. Cell. Biol. 24, 9383–9389.

Joseph, E.M., Melton, D.A., 1998. Mutant Vg1 ligands disrupt endoderm and mesoderm formation in *Xenopus* embryos. Development 125, 2677–2685.

Kiecker, C., Niehrs, C., 2001. The role of prechordal mesendoderm in neural patterning. Curr. Opin. Neurobiol. 11, 27–33.

Kirby, M.L., Lawson, A., Stadt, H.A., Kumiski, D.H., Wallis, K.T., McCraney, E., Waldo, K.L., Li, Y.X., Schoenwolf, G.C., 2003. Hensen's node gives rise to the ventral midline of the foregut: implications for organizing head and heart development. Dev. Biol. 253, 175–188.

Kontges, G., Lumsden, A., 1996. Rhombencephalic neural crest segmentation is preserved throughout craniofacial ontogeny. Development 122, 3229–3242.

Lowe, L.A., Yamada, S., Kuehn, M.R., 2001. Genetic dissection of nodal function in patterning the mouse embryo. Development 128, 1831–1843.

Monuki, E.S., Walsh, C.A., 2001. Mechanisms of cerebral cortical patterning in mice and humans. Nat. Neurosci. 4 Suppl., 1199–1206.

Nomura, M., Li, E., 1998. Smad2 role in mesoderm formation, left–right patterning and craniofacial development. Nature 393, 786–790.

Norris, D.P., Robertson, E.J., 1999. Asymmetric and node-specific nodal expression patterns are controlled by two distinct cis-acting regulatory elements. Genes Dev. 13, 1575–1588.

Norris, D.P., Brennan, J., Bikoff, E.K., Robertson, E.J., 2002. The Foxh1-dependent autoregulatory enhancer controls the level of Nodal signals in the mouse embryo. Development 129, 3455–3468.

Oh, S.P., Li, E., 1997. The signaling pathway mediated by the type IIB activin receptor controls axial patterning and lateral asymmetry in the mouse. Genes Dev. 11, 1812–1826.

Oh, S.P., Li, E., 2002. Gene-dosage-sensitive genetic interactions between inversus viscerum (iv), nodal, and activin type IIB receptor (ActRIIB) genes in asymmetrical patterning of the visceral organs along the left–right axis. Dev. Dyn. 224, 279–290.

Petryk, A., Anderson, R.M., Jarcho, M.P., Leaf, I., Carlson, C.S., Klingensmith, J., Shawlot, W., O'Connor, M.B., 2004. The mammalian twisted gastrulation gene functions in foregut and craniofacial development. Dev. Biol. 267, 374–386.

Rankin, C.T., Bunton, T., Lawler, A.M., Lee, S.J., 2000. Regulation of left–right patterning in mice by growth/differentiation factor-1. Nat. Genet. 24, 262–265.

Reissmann, E., Jornvall, H., Blokzijl, A., Andersson, O., Chang, C., Minchiotti, G., Persico, M.G., Ibanez, C.F., Brivanlou, A.H., 2001. The orphan receptor ALK7 and the Activin receptor ALK4 mediate signaling by Nodal proteins during vertebrate development. Genes Dev. 15, 2010–2022.

Rivera-Perez, J.A., Mallo, M., Gendron-Maguire, M., Gridley, T., Behringer, R. R., 1995. Goosecoid is not an essential component of the mouse gastrula organizer but is required for craniofacial and rib development. Development 121, 3005–3012.

Roessler, E., Muenke, M., 2001. Midline and laterality defects: left and right meet in the middle. BioEssays 23, 888–900.

Rossant, J., Tam, P.P., 2004. Emerging asymmetry and embryonic patterning in early mouse development. Dev. Cell 7, 155–164.

Shi, Y., Massague, J., 2003. Mechanisms of TGF-beta signaling from cell membrane to the nucleus. Cell 113, 685–700.

Skromne, I., Stern, C.D., 2001. Interactions between Wnt and Vg1 signalling pathways initiate primitive streak formation in the chick embryo. Development 128, 2915–2927.

Song, J., Oh, S.P., Schrewe, H., Nomura, M., Lei, H., Okano, M., Gridley, T., Li, E., 1999. The type II activin receptors are essential for egg cylinder growth, gastrulation, and rostral head development in mice. Dev. Biol. 213, 157–169.

Stern, C.D., 2001. Initial patterning of the central nervous system: how many organizers? Nat. Rev., Neurosci. 2, 92–98.

Tam, P.P., Beddington, R.S., 1992. Establishment and organization of germ layers in the gastrulating mouse embryo. Ciba Found. Symp. 165, 27–41.

Varlet, I., Collignon, J., Norris, D.P., Robertson, E.J., 1997a. Nodal signaling and axis formation in the mouse. Cold Spring Harbor Symp. Quant. Biol. 62, 105–113.

Varlet, I., Collignon, J., Robertson, E.J., 1997b. nodal expression in the primitive endoderm is required for specification of the anterior axis during mouse gastrulation. Development 124, 1033–1044.

Vincent, S.D., Dunn, N.R., Hayashi, S., Norris, D.P., Robertson, E.J., 2003. Cell fate decisions within the mouse organizer are governed by graded Nodal signals. Genes Dev. 17, 1646–1662.

Wall, N.A., Craig, E.J., Labosky, P.A., Kessler, D.S., 2000. Mesendoderm induction and reversal of left–right pattern by mouse Gdf1, a Vg1-related gene. Dev. Biol. 227, 495–509.

Yamada, G., Mansouri, A., Torres, M., Stuart, E.T., Blum, M., Schultz, M., De Robertis, E.M., Gruss, P., 1995. Targeted mutation of the murine goosecoid gene results in craniofacial defects and neonatal death. Development 121, 2917–2922.

Yamamoto, M., Meno, C., Sakai, Y., Shiratori, H., Mochida, K., Ikawa, Y., Saijoh, Y., Hamada, H., 2001. The transcription factor FoxH1 (FAST) mediates Nodal signaling during anterior–posterior patterning and node formation in the mouse. Genes Dev. 15, 1242–1256.

Yeo, C., Whitman, M., 2001. Nodal signals to Smads through Cripto-dependent and Cripto-independent mechanisms. Mol. Cell 7, 949–957.

Zakin, L., De Robertis, E.M., 2004. Inactivation of mouse Twisted gastrulation reveals its role in promoting Bmp4 activity during forebrain development. Development 131, 413–424.